PHYSICAL REVIEW B VOLUME 27, NUMBER 2 15 JANUARY 1983

Time-differential perturbed angular-correlation-technique studies of internal oxidation of impurities in silver

A. F. Pasquevich, F. H. Sánchez, A. G. Bibiloni,
J. Desimoni, and A. López-García
Departamento de Física, Facultad de Ciencias Exactas, Universidad Nacional de La Plata, 1900 La Plata, Argentina
(Received 12 April 1982)

The first quantitative results on internal oxidation of impurities in a noble-metal host, using the time-differential perturbed angular-correlation technique, are reported here. The system studied was indium-silver, with a few ppm of indium. The existence of a well-defined oxidation front is found for this highly dilute alloy. The kinetics of oxidation were determined for oxidating temperatures of 400 and 500 °C. Our results are in good agreement with a parabolic dependence of the depth of the internal oxidation front on the elapsed oxidation time. No unique indium-oxygen configurations were found in the range 280–900 °C.

I. INTRODUCTION

Some alloys undergo internal oxidation processes during annealing treatments in the presence of oxygen, i.e., besides a possible external scale of oxide of the alloy components, an internally oxidized zone can be observed, where oxidized solute particles appear embedded in the matrix. The existence of this zone mainly depends on the solubility of oxygen in the alloy and on the higher free energy of formation of the solute oxides. Optical microscopy observations[1] showed that there is a well-defined boundary between the internally oxidized zone and the alloy. This boundary, parallel to the metal surface, is called the oxidation front. Several authors[1–3] have interpreted the kinetics for the formation of the internal oxide in the absence of external scale. Experimental results are well described by their theory. Part of this evidence was obtained on silver-based alloys[4–9] but information about the behavior at low temperatures as well as on very diluted alloys is missing. To our knowledge, available values correspond only to oxidation temperatures higher than 450 °C and to concentrations of the oxidizable metal above 1%.

In recent publications[10,11] we showed that the time-differential perturbed angular correlation (TDPAC) technique is adequate to investigate the interactions between the nuclear quadrupole moment of the radioactive ions (probes) and the electric-field gradients existing at the sites of the metallic lattice. The electric-field gradient vanishes at those sites with cubic symmetry. In a cubic noble metal containing internal oxidation, the presence of the oxygen in the neighborhood of the probe (impurity ions) alters the charge distribution symmetry, creating an electric-field gradient. The information obtained experimentally is the perturbation factor which consists in this case of two components, one corresponding to the oxidized ions and the other to the nonperturbed ones. Their amplitudes are directly proportional to the respective ion fractions. In addition, from the interaction parameters it could be possible to identify the formed oxides. These parameters are the components of the electric-field gradient tensor at the site of the nuclei of the probe ions. Another advantage of this technique shared also by the residual-resistivity ratio (RRR) measurements[12] is the possibility of extending the internal oxidation studies to very diluted alloys. But in contrast to the RRR technique, the sensitivity of TDPAC technique is not reduced by the nonprecipitation of the oxides. In the following we present the first quantitative TDPAC results about the kinetic of internal oxidation of impurities in silver.

II. INTERNAL OXIDATION

The internal oxidation of alloys occurs due to the diffusion of oxygen in the base metal. An oxidation front is established at the depth $x=\xi$. As a result the free-oxygen concentration at depth $x \geq \xi$ is zero, and the concentration of the nonoxidized impurities $N_I(x,t)$ is zero for $x<\xi$. According to Wagner's theory,[2] if the oxidation process is controlled by dif-

fusion, the advance of the oxidation front is a parabolic function of the time t expressed as

$$\xi^2 = kt \ . \tag{1}$$

It is possible to establish a relation between the factor k in Eq. (1) and the parameters that rule the oxidation process. These are the oxygen concentration at the surface N_O^s (which according to Sievert's law depends on the square root of the oxygen partial pressure and on the temperature), the solute concentration in the alloy $N_I^0 = N_I(x,0)$, and the diffusion coefficients of oxygen D_O and of solute D_I in the alloy. In our case, where the relation

$$\frac{D_I}{D_O} \ll \frac{N_O^s}{N_I^0} \ll 1 \tag{2}$$

holds, the concentration changes are illustrated in Fig. 1. The value of the factor k in Eq. (1) is given, to a good approximation, by

$$k = \frac{2N_O^s D_O}{\nu N_I^0} \tag{3}$$

where ν is the number of oxygen atoms per solute atom in the oxide.

III. EXPERIMENTAL PROCEDURE

The ^{111}Cd used in the TDPAC measurements is obtained from the decay of ^{111}In ($\tau = 2.81$ d). The ^{111}In activity was produced by the ^{109}Ag(α,2n)^{111}In nuclear reaction on 99.99 at.% pure and 250-μm-thick silver-foil targets with 56-MeV α particles in the cyclotron of the Comisión Nacional de Energía

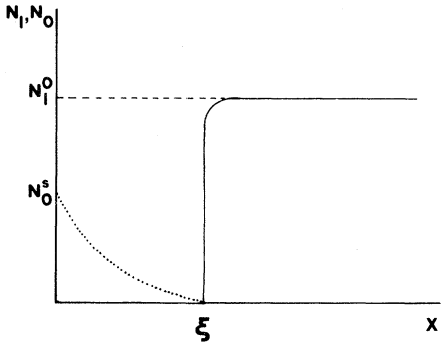

FIG. 1. Concentration profiles under the conditions of expression (2). The full line shows the concentration of unoxidized impurities and the dotted one the concentration of free oxygen. N_O^s is the oxygen concentration at the surface. N_I^0 is the impurity concentration in the alloy. Distances are measured from the surface. The oxidation front is located at $x = \xi$.

Atómica (CNEA), Buenos Aires. During irradiation other nucleides are also produced but almost all of them decay faster than ^{111}In. Since we wait about 24 h before collecting data, the only undesirable remaining activity is ^{106m}Ag ($\tau = 8.5$ d). The presence of ^{106m}Ag affects only the first two channels of the TDPAC spectra through the contribution of prompt cascades of its daughter ^{106}Pd. This contribution increases with time due to the longer half-life of ^{106m}Ag as compared to that of ^{111}In. We estimate that all these impurities amount to less than 50 ppm. The ^{111}In concentration determined from the activity remained always below 5 ppm.

In order to perform internal oxidation kinetic studies it is necessary to assure a uniform distribution of the indium activity (and that of the other impurities) as well as the absence of oxygen contamination. Both requirements were satisfied by melting the irradiated foils in quartz capsules filled with Ar at a pressure of 120-mm Hg. The resulting homogeneity was checked for some samples through γ radiation measurements as a function of the residual weight after successive etchings in HNO_3. The absence of oxygen contamination was verified by TDPAC measurements after thermal treatments in inert atmospheres.

After melting, the samples were rolled into foils whose widths were carefully measured. Typical dimensions were 150 mm$^2 \times 1$ mm. The oxidation treatments were performed under air in open quartz tubes in a conventional electric oven. The temperature was controlled by the use of a thermoelement in close contact with the samples. The temperature fluctuation was never larger than 2 °C. When the measurements were performed above room temperature an electrically heated quartz oven was used.

The TDPAC measurements were performed with the (173–247)-keV γ-γ cascade of ^{111}Cd. A conventional automatic two-detector apparatus, with one NaI(Tl) and one CsF scintillator, was used. The movable detector changed its position every 1800 s between $\theta = 90°$ and $\theta = 180°$ with respect to the fixed one.

The time spectra of coincidences $N(180°,t)$ and $N(90°,t)$ were stored in subgroups of a multichannel analyzer. We evaluated from these time spectra, corrected for accidental counts, the asymmetry ratio

$$R(t) = 2\frac{N(180°,t) - N(90°,t)}{N(180°,t) + 2N(90°,t)} \ ,$$

which is to good approximation (because the A_4 coefficient of this angular correlation can be

neglected) given by

$$R(t) \simeq A_2^{\text{expt}} G_2(t) ,$$

where A_2^{expt} is the measured angular correlation coefficient and $G_2(t)$ the perturbation factor, which contains the relevant information about the interaction between the nuclear quadrupole moment Q of the intermediate nuclear state and the principal component of the electric-field gradient V_{zz} at the nuclear site.

Theoretical functions of the form

$$G_2(t) = f_0 + f_1 \sum_{n=0}^{3} s_{2n} \exp(-\delta\omega_n t) \cos\omega_n t$$

folded with the measured time resolution curve (full width at half maximum of 2.4 ns) were fitted to the experimental data. Here f_0 is the fraction of nuclei at unperturbed lattice sites and f_1 the fraction of nuclei subject to the interaction characterized by the quadrupole frequency

$$\omega_Q = eQV_{zz} 2\pi / 40 \text{ h} ,$$

which is related to ω_n by $\omega_n = F_n(\eta)\omega_Q$. The coefficients F_n and s_{2n} are functions[13] of the axial asymmetry parameter η, defined by $\eta = (V_{xx} - V_{yy})/V_{zz}$. The exponential function accounts for a Lorentzian frequency distribution of relative width δ around ω_n.

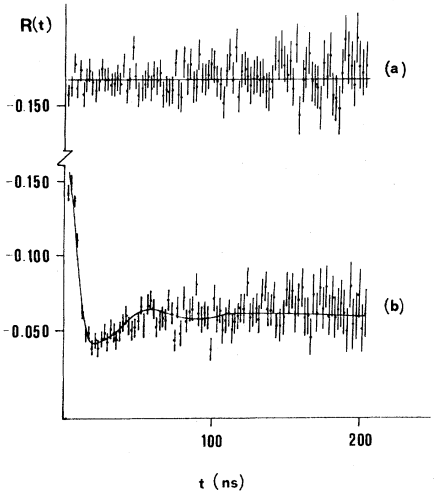

FIG. 2. $R(t)$ curves at room temperature. (a) after a treatment of 90 min at 450°C and 0.5 atm N_2, and (b) after a similar treatment in O_2. The full line shows the curve fitted to the data.

IV. RESULTS

Results obtained for one sample annealed under nitrogen and subsequently under oxygen atmospheres are shown in Figs. 2(a) and 2(b), respectively. It can be seen how the presence of the oxygen alters the cubic symmetry of the environment of a certain fraction of the probe nuclei. This fraction depends on the temperature and on the length of the oxidation treatment. However, neither the parameters that characterize the interaction (ω_Q and η) nor the distribution δ, seem to depend on the length of the treatment. In spite of some dispersion of the values of the parameters for each temperature a temperature dependence can be seen in Fig. 3, where we plot mean values of ω_Q and δ obtained from more than 60 measurements. Owing to the relatively large frequency distribution in the spectra, it is very hard to draw a conclusion from the fitted values for η.

In order to establish whether a sharp oxidation front exists (such as that described in Sec. II), in the case of very diluted alloys, the following experiment was done. One sample of 1-mm width was oxidized during 80 min at 500°C. The TDPAC results showed that 68% of the indium ions were oxidized. Two more TDPAC measurements were performed after two successive etchings with HNO_3. In Table I the values of the sample weights and widths and the fraction of oxidized ions determined after each etching are shown. From the 68% of oxidized ions found in the first measurement we calculated the depth ξ of the oxidation front assuming its existence, and taking into account that oxygen diffuses through both faces, from

$$\xi = fd/2 , \tag{4}$$

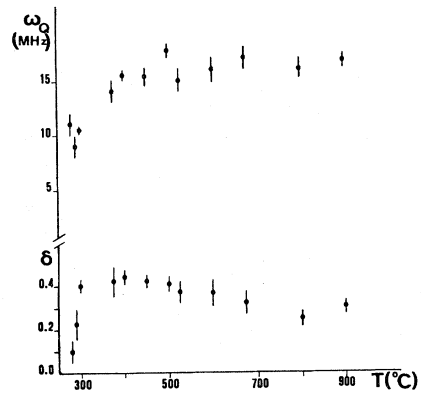

FIG. 3. Mean values for the interaction parameters ω_Q and δ, corresponding to several measurements at each temperature.

TABLE I. The weights are given just to give an idea of the size of the samples. The first value of ξ is calculated from Eq. (4) and the others according to the loss of mass after each etching. f(estimated) is calculated from Eq. (4).

m (g)	d (mm)	ξ (mm)	f(estimated) (%)	f(measured) (%)
1.540_1	1.000_1	0.340_{10}		68_2
0.819_1	0.650_1	0.165_{10}	51_3	50_2
0.408_1	0.327_1	0.003_{10}	0_4	0_3

where the penetration through the edges of the sample is neglected. This value and those corresponding to ξ after the successive etchings are also shown in Table I, as well as the remaining fractions of oxidized ions calculated from them. Within the sensitivity of the method and taking into account the approximation done in the calculation, the agreement is excellent.

In order to investigate the evolution of the oxidized ion fraction with the duration of the oxidation processes, sequences of oxidation treatments at 400 and 500 °C were performed. Figure 4 shows the sequence of the TDPAC spectra at 500 °C. The f_1 values obtained for each temperature are shown in Fig. 5 as a function of $t^{1/2}$. A least-squares fit of a straight line to the data gives 0.0440_{29} and 0.0550_{42} for the slopes at 400 and 500 °C, respectively. A parabolic dependence of the progression of the oxidation front is apparent. In fact, a least-squares fit of the expression $f=\alpha t^m$ to the experimental data yields respectively $m_{400}=0.53_4$ and $m_{500}=0.49_4$. The different values of the slopes in Fig. 5 are connected to the different oxidation temperatures, sample width, and purity. This arises from Eqs. (1), (2), and (4). From these slopes we estimate the νN values involved in both oxidation processes. To do this we calculated the diffusion coefficient D_O for oxygen in silver using 3.66×10^{-3} cm^2/s for the frequency factor and 45 980 J/mol for the activation energy as given in Ref. 14. Also the oxygen concentration N_O^s was calculated using 49 575 J/mol for the activation energy and 6.69×10^{-2} atoms oxygen per total atoms for the pre-exponential factor as given in Ref. 14, appropriately corrected using Sievert's law. In this way we obtained

$$\nu N=1.8_2\times10^{-4},$$

$$\nu N=4.7_7\times10^{-4}$$

for 400 and 500 °C, respectively; the units of νN being bonded oxygen atoms per initial alloy atoms in the oxidized zone. These different values may be attributed to different oxide stoichiometries (different ν) or to the fact that more impurities can be oxidized at the higher temperature.

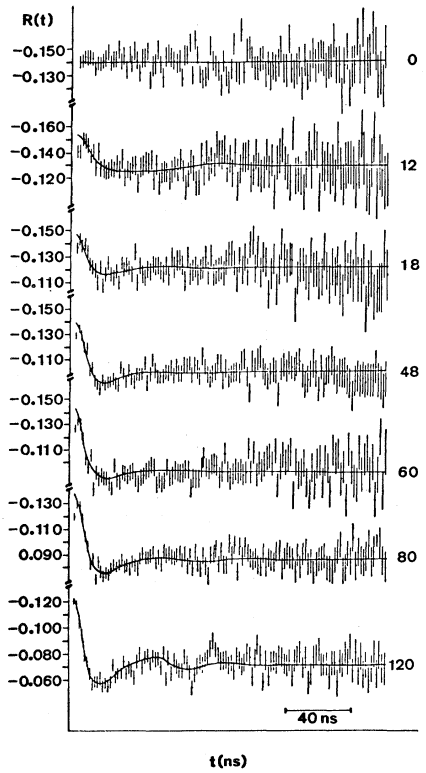

FIG. 4. TDPAC spectra after successive oxidation treatments at 500 °C. All measurements were done at room temperature. The cumulative oxidation time, in minutes, is indicated. Full lines show the curves fitted to the data.

V. DISCUSSION AND CONCLUSIONS

In the previous sections we have indicated that the presence of the oxygen in the neighborhood of

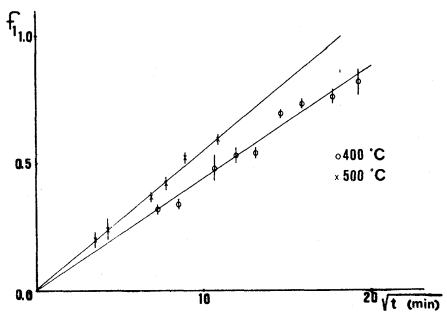

FIG. 5. Fraction f_1 of oxidized ions obtained for 400 and 500 °C as a function of $t^{1/2}$.

the indium ion is responsible for the observed electric quadrupole interaction. We can now argue about which kind of In-O complexes are formed. The behavior of the interaction frequency shown in Fig. 3 suggests that above 400 °C these complexes have a different nature than those formed below 300 °C. Although indium can form different oxides, TDPAC measurements have been performed only for In_2O_3 (Refs. 15 and 16) and show like ours a high attenuation. Salomon[16] reports a well-defined static interaction ($\omega_Q \simeq 30$ MHz) only if the measurement is performed at 280 °C. Though we do not expect formation of In_2O_3 due to the high indium dilution of our samples and the high velocity of the oxidation front, we carried out measurements on a sample fully oxidized at 450 °C at the following measurement temperatures: 280, 450, and 610 °C, but we did not observe the removal of the attenuation. The high distribution we measured could be explained taking into account the building up of In-O-Ag complexes. These complexes may involve different numbers of oxygen ions, with the indium ion, perhaps, shifted from its original substitutional position and with electronic bonds of different character as suggested by Huffman and Podgurski for the internal oxidation of Sn in silver.[9]

From our experimental results there is evidence of the existence of an oxidation front in the case of these very dilute alloys. The parabolic rate of the internal oxidation has been shown for 400 and 500 °C. From the νN values given in Sec. IV not very much can be said, since ν is a mean value over all oxidized impurities. But the method is capable of giving information about the number of oxygen atoms per solute once there is prevailingly one kind of oxide. Therefore, experiments at different temperatures are being carried out to determine the stoichiometry of the oxides in 1% In*Ag* alloys.

ACKNOWLEDGMENTS

We wish to acknowledge the cyclotron staff of the CNEA for the irradiation facilities. Our work was partially supported by Consejo Nacional de Investigaciones Científicas y Técnicas (CONICET), Secretaría de Estado de Ciencia y Tecnología (SECYT), Comisión de Investigaciones Científicas de la Provincia de Buenos Aires (CICPBA), and Kernforschungszentrum Karlsruhe Gesellschaft mit beschränkter Haftung.

[1]F. N. Rhines, Trans. AIME 137, 246 (1940).
[2]C. Wagner, J. Electrochem. Soc. 63, 777 (1959).
[3]L. S. Darken, Trans. AIME 150, 147 (1942).
[4]F. N. Rhines and A. H. Grobe, Trans. AIME 147, 318 (1942).
[5]J. L. Meijering and M. J. Druyvesteyn, Philips Res. Rep. 2, 81 (1947).
[6]I. Dietrich and L. Koch, Z. Metallkd. 50, 31 (1959).
[7]R. A. Rapp, Acta Metall. 9, 730 (1961).
[8]J. E. Verfurth and R. A. Rapp, Trans. AIME 230, 1310 (1964).
[9]G. P. Huffman and H. H. Podgurski, Acta Metall. 21, 449 (1973).
[10]A. F. Pasquevich, F. H. Sanchez, A. G. Bibiloni, C. P. Massolo, and A. López-García, in *Nuclear and Electron Resonance Spectroscopies Applied to Materials Science,* edited by E. N. Kaufmann and G. K. Shenoy (North-Holland, Amsterdam, 1981), p.435.
[11]A. F. Pasquevich, A. G. Bibiloni, C. P. Massolo, F. H. Sánchez, and A. López-García, Phys. Lett. 82A, 34 (1981).
[12]A. C. Ehrlich, J. Mater. Sci. 9, 1064 (1974).
[13]L. A. Mendoza-Zélis, A. G. Bibiloni, M. C. Caracoche, A. López-García, J. A. Martinez, R. C. Mercader, and A. F. Pasquevich, Hyp. Interact. 3, 315 (1977).
[14]W. Eichenauer and G. Müller, Z. Metallkd. 53, 321 (1962); 53, 700 (1962).
[15]P. Lehman and J. Miller, J. Phys. Radium 17, 526 (1956).
[16]M. Salomon, Nucl. Phys. 54, 171 (1964).